Narrowband Interference Suppression in Long Term Evolution Systems

João Paulo Miranda, Dick Melgarejo, Fabiano Mathilde,
Ricardo Yoshimura, Felipe Augusto de Figueiredo, and Juliano João Bazzo
Centre for Research and Development in Telecommunications (CPqD), Campinas/SP, Brazil
Email: [jmiranda, dickm, fabianom, rseiti, felipep, jbazzo]@cpqd.com.br

***Abstract*—Narrowband interference (NBI) is a known problem in wireless communications. However, analyses found in the NBI literature often model the signal of interest as a generic transport channel with all subcarriers conveying information of the same kind, $e.g.$ user plane data. By taking the analysis down to physical channels' level, this paper aims to obtain a deeper understanding of the impact exerted by NBI on *both* the user *and* control planes of Long Term Evolution (LTE) systems. First, field measurements are carried out to characterize the narrowband systems operating in the recently standardized LTE Band 31 (450-470 MHz). On the basis of these findings, requirements for NBI suppression in the LTE downlink are established. Some prominent time-frequency distributions (TFDs) are then evaluated via computer simulations with respect to their ability to fulfill such requirements. Among the TFDs considered, wavelets offer the best compromise in terms of complexity and signal distortion regardless the type of physical channel. For those cases where information about the NBI center frequencies is not available a priori, we propose a blind time-domain canceller based on the Wigner-Ville distribution.**

I. Introduction

Narrowband interference (NBI) is the interference caused by a narrowband wireless communication system on another wireless communication system that uses wideband or spectrally spread signals. The effects of NBI manifest themselves when a wideband receiver within the coverage area of a narrowband transmitter does *not* pick up noisy signals of interest (SOI), *but* a sum of SOI, narrowband signals and noise instead. Depending on the transmit power of the narrowband system, the undesired components present in the sum signal may introduce nonlinear distortions in the automatic gain control and analog-to-digital conversion blocks of the wideband receiver. This is a well understood issue and ways to tackle it are known for NBI of both non-intentional nature [1]–[6], and of intentional nature [7], [8], $e.g.$ jamming in military communications.

NBI suppression techniques commonly have as basis some sort of three-step process. The first step is the decomposition of the received signal into a transform domain where narrowband components can be more easily identified. These components are estimated and subsequently removed from the received signal in the second step. In case SOI and narrowband signals are distinguishable in the selected domain, the components due to the latter can be estimated using maximum likelihood (ML) [1], linear minimum mean square error (MMSE) [2], or a combination of compressive sensing and weighted least squares [3]. Finally, the third step applies the corresponding inverse transform to the remaining signal components. This reconstructs the noisy SOI, thus bringing the solution back to the original problem domain.

Excision approaches exploit the fact that NBI often comes into play as high-power signals that can be distinguished from lower-power SOI in the frequency domain. Robustness against narrowband signals with center frequencies that change over time, and frequency selective fading are among their advantages. However, when the NBI spectra do not sit at frequencies coinciding with the bins of the discrete-time Fourier transform (DFT), carried out at the demodulator, spectral leakage occurs. The higher the NBI power, the larger the number of corrupted subcarriers in the reconstructed signal. Such signal distortion can be mitigated by mapping the data only to those subcarriers whose powers exceed a given signal-to-interference ratio [4]. A drawback of this approach is that the use of weighted-type fractional Fourier transforms results in a system that may fail to comply with currently DFT-based wireless standards.

Techniques that operate in the time domain avoid spectral leakage by applying cancellation filters before the DFT block. Time-domain cancellers require less prior knowledge to work than their frequency-domain counterparts, $e.g.$ only estimates of the frequencies where the NBI spectrum sits at and/or its power per subcarrier. As for the limitations, performance may deteriorate in the presence of frequency offsets. This is exactly the case with phase-locked loops [5], which may undergo a further drop in performance if quadrature phase shift keying (QPSK) is in use. Care must also be taken when it comes to filter design, as impulse responses longer than the SOI's cyclic prefix (CP) introduce intersymbol interference (ISI).

In general, NBI suppression in frequency *and* time domains offer flexibility and resolution superior to those obtained in a single domain. Time-frequency distributions (TFDs), such as wavelet transforms [6], multirate digital filter banks (MDFBs) [7], and bilinear signal distributions [8], are tools of relatively lower complexity and allow near-perfect signal reconstruction at the cost of none or very few prior knowledge of the systems and signals causing NBI. Another advantage is that, by direct representing the frequency content of the signal while keeping the time description parameter, the linear progression of the frequency with time can be clearly observed [9]. Despite its potential for providing robustness against NBI, the application of TFDs has been limited to spectrally spread systems [6]–[8] and a better understanding on how these tools perform in the context of multicarrier wideband systems is needed.

Motivated by real-world conditions characterized via field measurements, we assess in this paper the performance of some prominent TFDs as means for suppressing NBI in Long Term Evolution (LTE) physical channels. On the basis of the characteristics of narrowband sources and signals found in a standard LTE band, we establish a set of design requirements for NBI suppression (Section II). These drive the definition of a proper system model (Section III), and the set up of parameters specific to each TFD under analysis for the simulation work (Section IV). Conclusions are drawn in Section V.

II. Motivation

To characterize the NBI a LTE system may be subject to, we carried out field measurements in the 450-470 MHz range. The reason why we have chosen these frequencies is two-fold. The first reason has its roots in the Brazilian National Broadband Plan (BNBP), which in May 2010 advanced the use of the 225-470 MHz range to accommodate new broadband services [10]. BNBP's goal is to increase the penetration rates of broadband services, especially in the countryside and remote areas where a significant number (≈30 millions) of Brazilians live. Later in that same year, the Brazilian Regulatory Agency (ANATEL) allocated the 451-458 MHz and 461-468 MHz bands as uplink and downlink, respectively, for fixed and mobile radio services operating in frequency division duplex mode [11].

The second reason relates to the standardization of the 450 MHz band, designated as Band 31, by the Third Generation Partnership Project (3GPP) [12]. 3GPP's aim is to benefit from the superior propagation characteristics of lower frequencies in a new LTE profile for fourth generation systems operating in sparsely populated areas. On behalf of the Brazilian Ministry of Communications, CPqD supported 3GPP in the determination of appropriate channelization schemes, coexistence solutions, and transceiver radio parameters. These specifications will soon become available as part of LTE Release 12.

A. Characterization of NBI Sources & Signals

In Brazil, the Band 31 is predominantely assigned to voice services, whose channels are 12.5 kHz wide. The resolution of the spectrum analyzer was therefore set to 3 kHz, for 5 MHz (SOI) segments, and 0.3 kHz, for 12.5 kHz (NBI) segments. The antenna selected for the measurements was a custom-built J-pole antenna made of 15 mm copper tubes. A laptop running the software LabView allowed sample processing and storage to be carried out in an automated fashion. In the discussion that follows, we analyze the findings obtained using this setup in a measurement campaign carried out in Campinas, São Paulo. The exact measurement site coordinates and height above the terrain were 22°54'S 47°02'W and 667 m, respectively.

An analysis of the cumulative distribution function (CDF) of received power per segment revealed that, for most segments, the NBI power lies below the noise floor (due to the typically higher sensitivity of narrowband radios). However, high-power NBI (-65 dBm and above) was found sitting at f_1 = 463.5500 MHz, f_2 = 464.6000 MHz, f_3 = 457.5375 MHz, and f_4 = 469.1625 MHz. According to [13], a search tool publicly made available by ANATEL, the first three frequencies are granted

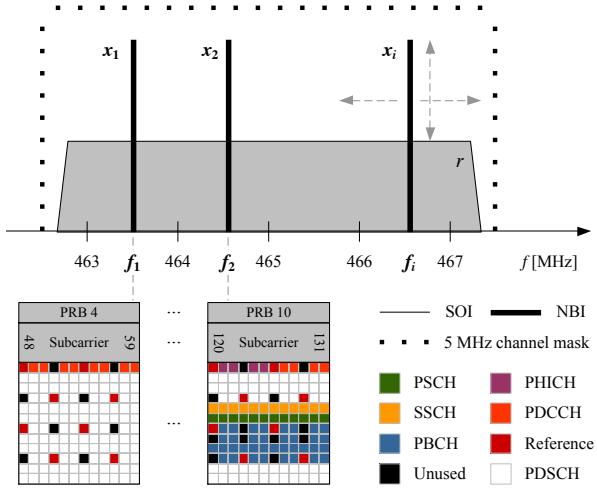

Fig. 1. Exemplary scenario of NBI in the LTE downlink. The signals x_1 and x_2 are real-world narrowband signals found in the Band 31. The signal x_i is an artificially-created narrowband signal that introduces controlled NBI.

to push-to-talk (PTT) systems used for highway control and oil & gas purposes. The fourth one is granted to the city town of Campinas for data transmissions. Another CDF analysis, now in terms of talk time, showed that PTT communications last up to 20 seconds for 90% of the cases. The segment occupation was also found to lie around 30% on average, for PTT signals, and 100% of the time, for data signals.

Our measurements confirmed the presence of multiple narrowband systems in both uplink and downlink frequencies designated for the operation of LTE 450 MHz systems. Building on these findings, we can set requirements for NBI suppression so as to ascertain coexistence between LTE and narrowband systems[1]. Before we proceed, note that f_4 is about ten resource blocks (RB) away from the LTE subcarrier conveyed by the highest frequency in the downlink. This is far enough for the corresponding data-based narrowband signals not to interfere with the LTE system. NBI suppression in the uplink is out of the scope of this paper[2], so the PTT-based narrowband signals sitting at f_3 will not be taken into consideration.

As depicted in Figure 1, the remaining narrowband signals x_1 and x_2 overlap different portions of r, the signal received in the LTE downlink: x_1 mainly affects data on the user plane, $i.e.$ the physical downlink shared channels (PDSCH), while x_2 mainly affects control plane information. In particular, x_2 has potential to disrupt the Zadoff-Chu sequences conveying symbol timing and frequency offsets in the primary synchronization channels (PSCH). If so the receiver fails to get time synchronized with the system, thus making it hard to extract frame timing and cell identity information transmitted in the

[1] Although such need for coexistence is clear in the context considered here, it may well be justified also in any other bands and/or locations where legacy (non-LTE) systems are in the process of being refarmed.

[2] Our field measurements suggest that the impact of NBI is more detrimental in the downlink because of its potential to cause the user terminal to loose connectivity with the base station, as explained later. An uplink analysis along the same lines used here should be straightforward to obtain.

secondary synchronization channels (SSCH). The lack of the aforementioned information prevents the correct access on the part of the receiver to basic operation parameters, such as channel bandwidth, CP length, and antenna mode, transmitted in the physical broadcast channels (PBCH). As a consequence, the cell search procedure gets compromised and the receiver cannot register with the cell [14].

B. Requirements for NBI Suppression in the LTE Downlink

In light of the above discussion, we conclude that candidate solutions for NBI suppression in the LTE downlink should be designed having the following requirements in mind:

- Low signal distortion: LTE operation occurs most of the time (up to 70%) in the absence of high-power NBI. Near-perfect signal reconstruction is crucial to maintain the bit error rate (BER) of the system.
- Prior knowledge: For flexibility and practical feasibility, the amount of information known a priori about narrowband signals should be kept as low as it can possibly be, $i.e.$ blind techniques are preferred.
- Low computational complexity: Narrowband systems currently found in LTE operation bands may not be refarmed, nor undergo modifications of any kind soon. NBI originated from these systems can be suppressed at the receive side, where low-complex approaches are preferred.

III. System Model

Let N_{S} denote the number of subcarriers, $C_f(e)$ the complex constellation transmitted by the eth subcarrier during the fth symbol, Δf the subcarrier spacing, T_{CP} the length of the cyclic prefix, T_{S} the sampling period. The LTE downlink Orthogonal Frequency-Division Multiplexing (OFDM) signal conveyed by the fth symbol is given by

$$s(t) = \sum_{e=-\lfloor N_{\mathrm{S}}/2 \rfloor}^{\lceil N_{\mathrm{S}}/2 \rceil} C_f(e) \exp\left(j2\pi\Delta f e(t - T_{\mathrm{CP}} T_{\mathrm{S}})\right), \quad (1)$$

where each RB is formed by grouping F consecutive symbols into a block of E consecutive subcarriers, and $C_f(0) = 0$. The resource grid, physical signals and channels are then generated in detailed accordance to the standard [15]. In what follows, by abuse of notation, we shall refer to (1) as the SOI associated with a generic but standard-compliant LTE physical channel.

Suppose the SOI now becomes corrupted by $i = 0, \ldots, I$ narrowband signals. The NBI sources statistically relevant (in terms of transmit power and talk time) in the Band 31 were earlier shown to be PTT radios. The signals transmitted within such systems can be assumed, without loss of generality, based on frequency modulation (FM). Under this assumption, the FM signal transmitted by the ith NBI source can be written as

$$x_i(t) = A_i \cos\left[2\pi f_i t + 2\pi f_{\mathrm{dev}} \int_0^t a_i(u)du + \theta_i\right], \quad (2)$$

where A_i, f_i, and f_{dev} are the magnitude, center frequency, and frequency deviation of the carrier used to modulate the audio signal $a_i(t)$, and the random phase θ_i is uniformly distributed in the interval $(0, 2\pi)$.

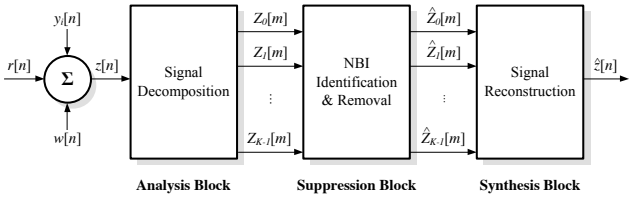

Fig. 2. Block diagram of a generic NBI suppression process.

After being passed through a multipath fading channel with impulse response $h[l]$ and L taps, the signal picked up by the LTE receiver (assumed not desensitized) corresponds to

$$z[n] = r[n] + \sum_{i=0}^{I} y_i[n] + w[n], \quad (3)$$

where $r[n]$ and $y_i[n]$ are filtered versions of (1) and (2), $i.e.$ $r[n] = \sum_{l=0}^{L-1} h[l]s[n - \sigma_l]$ and $y_i[n] = \sum_{l=0}^{L-1} h[l]x_i[n - \sigma_l]$, σ_l is the channel delay spread associated with the lth channel tap, and $w[n]$ is additive white Gaussian noise (AWGN) statistically independent from tap to tap. Note that, in contrast to the static (and probably band specific) NBI scenario discussed in Section II, the narrowband signals modeled by (2) and (3) can vary in number, power, and position. This allows the different LTE downlink physical channels to be fully exercised in the absence or presence of controlled NBI.

Most NBI suppression techniques have as their basis some sort of three-step process. The first step is the decomposition of $z[n]$, a sum of SOI, NBI and noise, into some transform domain where the signal components corresponding to the NBI are "easier" to identify. The second and third steps respectively involve the removal of such undesired components, and the reconstruction of an estimate of $z[n]$, $\hat{z}[n]$. A generic representation of this process is given in Figure 2. The analysis block outputs a set of channels $Z_k[m]$, $k = 0, 1, \ldots, K-1$, which are fed into a suppression block. After the narrowband signals $y_i[n]$ have been estimated and cancelled out, $\hat{Z}_k[m]$, $k = 0, 1, \ldots, K-1$, channels are made available for the synthesis block. To keep signal distortion low, the reconstructed signal $\hat{z}[n]$ should provide a good approximation of (3) when $I = 0$, $i.e.$ the no NBI case.

In the sequel, we make a brief recall on TFDs with potential to meet the requirements specified in Section II. Consistency with Figure 2 will be maintained to the extent possible.

A. Multirate Digital Filter Banks

MDFBs can be used to represent discrete-time signals based on short-time Fourier analysis, while avoiding the drawbacks ($e.g.$ poor resolution) of the latter. However, the processing in each of the K channels of the bank of filters is redundant, and the order of the lowpass filters is often high. If the channels are uniformly and contiguously spaced, and critically sampled, a more efficient option is to decompose $z[n]$ using [7]

$$Z_k[m] = \sum_{\rho=0}^{M-1} \sum_{r=-\infty}^{\infty} \bar{p}_\rho[r] z_\rho[m - r] W_M^{-k\rho}, \quad (4)$$

where the sample index m may differ from n, the decimation and interpolation ratio M is equal to K, $\bar{p}_\rho[m] = h_\mathrm{A}[mM-\rho]$ is the ρth polyphase branch of lowpass analysis filter $h_\mathrm{A}[n]$, $r = [n+\rho]/M$, and $W_M = \exp(j2\pi)/M$. Signal reconstruction can be efficiently implemented using

$$\hat{z}_\rho[r] = \frac{1}{M}\sum_{k=0}^{M-1}\sum_{m=-\infty}^{\infty} q_\rho[r-m]\hat{Z}_k[m]W_M^{k\rho}, \qquad (5)$$

where $q_\rho[m] = h_\mathrm{S}[mM+\rho]$ denotes the ρth polyphase branch of lowpass synthesis filter $h_\mathrm{S}[n]$. A parallel implementation of sets of filters $\bar{p}_\rho[m]$ and $q_\rho[m]$ is a *polyphase network*, and the polyphase structures in (4) and (5) are mathematically equivalent to the banks of lowpass filters and decimators/interpolators that would result from the direct mechanization of analysis and synthesis blocks based on MDFBs.

B. Wavelet Transforms

Filter banks play a central role also in the area of wavelets due to their close relationship with the discrete wavelet transform (DWT). Implementation of the analysis (synthesis) block using the DWT requires only a lowpass filter and a highpass filter, whose outputs are both downsampled (upsampled) by 2. The multilevel DWT involves the repetitive application of uniform filter banks on the low-frequency channel, meaning that redundancy is introduced more in that channel as compared to the high-frequency channel. In such multilevel settings, finer resolution is achieved but the recursive coefficient computation raises the need to store intermediate coefficients. This burden can be avoided by replacing the cascaded lowpass filters and subsampling by 2 at each resolution level of the analysis block by an equivalent analysis filter, defined in the z-domain as [16]

$$H_\mathrm{A}^J(z) = \prod_{j=0}^{J-1} H_\mathrm{A}(z^{2^j}). \qquad (6)$$

An equivalent synthesis filter $H_S^J(z)$ can be generated accordingly to replace the cascaded highpass filters and upsampling by 2 used in the synthesis block. In either case, the coefficients of the jth level can now be computed without prior knowledge of the coefficients of the $(j-1)$th level.

C. Bilinear Signal Distributions

A filter bank is also a special quadratic TFD that represents the signal in a joint time-frequency domain. Among bilinear TFDs, the representation regarded as the most powerful and fundamental is the *Wigner-Ville distribution* (WVD) due to the superior covariance properties it possesses. The discrete-time WVD (DWVD) can be written as [17]

$$Z_k[n] = \sum_{r=-N}^{N} z[n+m]z^*[n-m]w[m]w^*[-m]W_4^{km}, \quad (7)$$

where the window $w[m] = 0$ for $|m| > N$, $N \in \mathbb{Z}$, and $W_4 = \exp(-j4\pi/K)$. The additional power of 2 in W_4 is a scaling in frequency that is negligible, so it can be replaced by the standard twiddle factor $W_2 = \exp(-j2\pi/K)$ used in the DFT. Different synthesis procedures can be employed to obtain the reconstructed signal $\hat{z}[n]$ [18], but they are somewhat cumbersome to implement in practice. We therefore decided to exploit the superior visualization of DWVD-based analysis in a simple time-domain NBI canceller. Since SOI subcarriers are all transmitted at the same power level for a given modulation scheme and data traffic, the indices of subcarriers corrupted by NBI can be *blindly* identified using the DWVD over the entire received signal bandwidth. Having confirmed the presence of in-band narrowband signals (which are clearly distinguishable from the SOI in the DWVD domain), we "blank" corrupted subcarriers in the time domain, bringing their gains back to the expected value. The blanking threshold used is computed on the basis of the average standard deviation of the power received over all subcarriers.

IV. Simulation Work

In this section, we discuss some preliminary results obtained using a custom-built Matlab simulator that implements the LTE PHY in detailed accordance to the standard [14][15]. The simulation settings common to all techniques and those that are technique-specific are both summarized in Table I. We conducted simulations for the cases 'NBI Off $(I = 0)$', 'NBI On $(I = 1)$' without suppression, and 'Technique', which means that NBI is suppressed using the corresponding technique. The latter two cases introduce NBI at f_1 = 463.5500 MHz and f_2 = 464.6000 MHz, one frequency at a time, so we can evaluate the impact on the performance of PDSCH and PSCH/SSCH. The NBI/SOI power ratio is 15 dB, which corresponds to the worst-case condition observed in our measurements.

3GPP has been developing channel models for LTE. However, to the best of our knowledge, no standardized (nor widely accepted) model reflecting LTE operation in the Band 31 was available at the time of writing. A suitable alternative, which meets most requirements mandated by ANATEL [11], is the 6-tap channel model established within the IEEE 802.22 standard [19]. In the sequel, we present a smaller set of results obtained using profile 'A', which has coherence bandwidth, maximum delay spread, and maximum Doppler frequency of 47.62 kHz, 21 μs, and 2.50 Hz, respectively. Upon passing through this channel, PTT and LTE signals will undergo flat and frequency-selective fading, respectively, but both signals will be subject to less destructive slow fading characteristics.

TABLE I
General & Specific Settings used in the Simulations.

SOI Parameters					
N_S	Δf	T_CP	$1/T_\mathrm{S}$	f_c	BW
512	15kHz	16.67μs	30.72MS/s	465MHz	5MHz
NBI Parameters					
A_i	f_i	f_dev	I	BW	
NBI/SOI=15dB	f_1, f_2	5kHz	$\{0, 1\}$	12.5kHz	
Parameters/Technique		**MDFBs**	**Wavelets**	**Bilinear**	
Type of implementation		Polyphase	Daubechies	DWVD	
No. of parallel channels, K		16	2 per level	512	
Decim./interpol. ratio, M		16	2	–	
No. of resolution levels, J		1	8	1	
Filter/window length, N		256 taps	16 taps	512 bins	

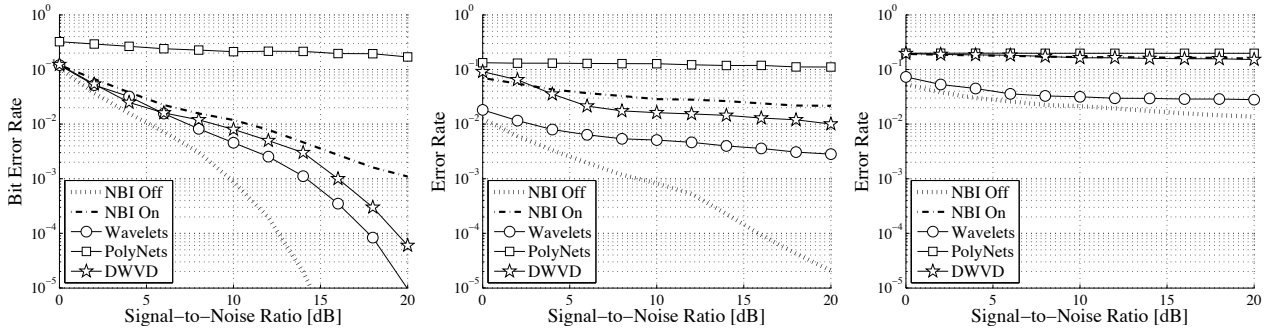

(a) PDSCH @$f_1 = 463.55$MHz (b) PSCH @$f_2 = 464.60$MHz (c) SSCH @$f_2 = 464.60$MHz

Fig. 3. Performance obtained over LTE physical channels using different NBI suppression techniques. User plane performance evaluated in (a) is characterized in terms of bit error rate, while control plane performance evaluated in (b) and (c) is characterized as a simple error rate.

Since the simulation is under multipath fading, the CP is set to extended ($T_{\text{CP}} = N_{\text{S}}/T_{\text{S}} \approx 16.67$ μs) and the modulation to QPSK with code rate 1/3. Antenna mode is SISO, channel estimation is assumed ideal, and equalization relies on MMSE. 5×10^7 Monte Carlo trials are carried out for each SNR point.

As seen in Figure 3, the best suppression results are obtained using wavelets regardless the physical channel type. This is in good agreement with our expectations because the resolution achieved by the 8-level DWT used is about 20 times finer than that of the 256-tap polyphase implementation, here referred to simply as 'PolyNets'. While the multilevel DWT is capable of cancelling out NBI in a highly localized fashion, PolyNets and our DWVD-based approach act on the entire SOI bandwidth. In fact, it turns out that the use of MDFBs for NBI suppression in systems with nonoverlapping designs is not advisable, as the attenuation outside the filters' stopband regions can never be infinite in practice. This harms the subcarrier orthogonality of OFDM (introducing signal distortions), thus explaining the poor perfomance of PolyNets observed here. Despite of being the best performer, the DWT needs to know the center frequencies where NBI sits at in order to suppress it. The simple DWVD-based approach proposed has also shown value, and its application can be considered as a blind alternative to wavelets when no such prior knowledge is available.

V. Concluding Remarks

This paper has analyzed the problem of NBI in the context of LTE. By taking a physical channels perspective, we provide a better understanding of the impact NBI exerts on the user and control planes of LTE downlink. Some prominent TFDs were evaluated via computer simulations with respect to their ability to fulfill a set of NBI suppression requirements determined on the basis of field measurements. Among the TFDs considered, wavelets offer the best compromise in terms of complexity and signal distortion regardless the type of physical channel. For those cases where knowledge of NBI center frequencies is not available a priori, we propose a blind time-domain canceller based on the Wigner-Ville distribution.

Acknowledgment

This material is based upon work supported by FUNTTEL/FINEP under grants 01.12.0481.00 and 01.09.0631.00. The authors would like to thank Dr. L. C. Pereira for fruitful discussions on the suitability of the 802.22 channel model for simulations in the 3GPP Band 31.

References

[1] M. E. Sahin, I. Guvenc and H. Arslan, "An Iterative Interference Cancellation Method for Co-channel Multicarrier and Narrowband Systems", *Physical Communication*, vol. 4, no. 1, pp. 13-25, Mar. 2011.

[2] R. Nilsson, F. Sjoberg and J. P. LeBlanc, "A Rank-Reduced LMMSE Canceller for Narrowband Interference Suppression in OFDM-based Systems", *IEEE Trans. Commun.*, vol.51,no.12,pp.2126-2140, Dec.2003.

[3] A. Gomaa and N. Al-Dhahir, "A Compressive Sensing Approach to NBI Cancellation in Mobile OFDM Systems", *In Proc. of the IEEE Globecom*, pp. 1-5, Dec. 2010.

[4] L. Mei, Q. Zhang, X. Sha and N. Zhang, "WFRFT Precoding for Narrowband Interference Suppression in DFT-based Block Transmission Systems", *IEEE Commun. Lett.*, vol.17, no.10, pp.1916-1919, Oct. 2013.

[5] A. J. Coulson, "Bit Error Rate Performance of OFDM in Narrowband Interference with Excision Filtering", *IEEE Trans. Wireless Commun.*, vol. 5, no. 9, pp. 2484-2492, Sept. 2006.

[6] F. Dovis and L. Musumeci, "Use of Wavelet Transforms for Interference Mitigation", *In Proc. of the ICL-GNSS*, pp. 116-121, June 2011.

[7] W. W. Jones and K. R. Jones, "Narrowband Interference Suppression using Filter-bank Analysis/Synthesis Techniques", *In Proc. of the IEEE Milcom*, vol. 3, pp. 898-902, Oct. 1992.

[8] Y. Zhang, M. G. Amin and A. R. Lindsey, "Anti-jamming GPS Receivers based on Bilinear Signal Distributions", *In Proc. of the IEEE Milcom*, pp. 1070-1074, Oct. 2001.

[9] F. Auger, P. Flandrin, P. Goncalves, and O. Lemoine, *Time Frequency Toolbox for Use with Matlab*, CNRS and Rice University, Oct. 2005.

[10] Brazilian Ministry of Communications, "A national plan for broadband: Brazil in high speed [in Portuguese]", 2009.

[11] Brazilian National Agency of Communications (ANATEL). Resolution No. 558, "Regulations on channelization and use conditions of radiofrequencies in the 450-470 MHz band [in Portuguese]", Dec. 2010.

[12] 3GPP TR 36.840, "LTE 450MHz in Brazil Work Item Technical Report", Sept. 2013.

[13] Brazilian National Agency of Communications (ANATEL). The STEL System [Online]. Available: http://sistemas.anatel.gov.br/stel/

[14] 3GPP TS 36.213, "Physical Layer Procedures", Sept. 2012.

[15] 3GPP TS 36.211, "Physical Channels and Modulation", Sept. 2012.

[16] K. K. Shukla and A. K. Tiwari, "Efficient Algorithms for Discrete Wavelet Transform with Applications to Denoising and Fuzzy Inference Systems", Springer 2013.

[17] B. Boashash and P. J. Black, "An Efficient Real-Time Implementation of the Wigner-Ville Distribution", *IEEE Trans. Acoust., Speech, Signal Process.*, vol. 35, no. 11, pp. 1611-1618, Nov. 1987.

[18] P. J. Kootsookos and B. Boashash, "Signal Synthesis in a Time-Frequency Domain using the Wigner-Ville Distribution", *In Proc. of the IREE Conference*, pp. 845-848, 1987.

[19] E. Sofer and G. Chouinard, "WRAN Channel Modeling", IEEE 802.22-05/0055r7, Sept. 2005.